Int. J. Heat Mass Transfer. Vol. 28, No. 10, pp. 1823–1830, 1985
Printed in Great Britain

0017–9310/85 \$3.00 + 0.00

Hyperbolic heat conduction with surface radiation

D. E. GLASS, M. N. ÖZIŞIK
Mechanical and Aerospace Engineering Department, North Carolina State University, Raleigh, NC 27695-7910, U.S.A.

and

BRIAN VICK
Mechanical Engineering Department, Virginia Polytechnic Institute and State University, Blacksburg, VA 24061, U.S.A.

(*Received* 4 *December* 1984 *and in final form* 1 *March* 1985)

Abstract—A numerical approach is used to solve hyperbolic heat conduction in a semi-infinite medium where the boundary at $x = 0$ is subjected to a surface heat flux and dissipates heat by radiation into an ambient at temperature T_∞. The results are compared with those obtained from the standard parabolic heat conduction equation.

INTRODUCTION

THE CLASSICAL parabolic heat conduction equation breaks down at temperatures near absolute zero, or at moderate temperatures when the elapsed time during a transient is extremely small. In such situations, the wave nature of thermal transport becomes dominant, hence a thermal disturbance travels in the medium with a finite speed of propagation. This is in contrast to the infinite speed of propagation predicted by the classical parabolic heat conduction equation. The non-Fourier heat flux equation leading to the hyperbolic heat conduction equation has been developed by several different approaches [1–7], and the existence of thermal waves propagating with a finite speed have been demonstrated experimentally [8, 9]. Since then, several analytic and numerical solutions of such problems have been reported [10–16]. All solutions that have been previously presented involve linear boundary conditions. In this work, numerical solutions are developed for hyperbolic heat transfer involving non-linear, radiation boundary conditions, and the results are compared with those obtained by the standard parabolic heat conduction equation. MacCormack's predictor–corrector method is used to perform the numerical computations for the hyperbolic equation, while a combined implicit/explicit method is used to solve the parabolic equation.

FORMULATION

A modified heat flux equation that accommodates the finite propagation speed of observed thermal waves was proposed by Vernotte [1] in the form

$$\tau \frac{\partial q(x,t)}{\partial t} + q(x,t) = -k \frac{\partial T(x,t)}{\partial x} \tag{1a}$$

where the relaxation time τ is defined as

$$\tau = \frac{\alpha}{c^2}. \tag{1b}$$

Here, α is the thermal diffusivity and c is the velocity of propagation of the thermal wave in the medium. Clearly, $\tau = 0$ leads to the classical Fourier equation,

$$q(x,t) = -k \frac{\partial T(x,t)}{\partial x} \tag{2}$$

which implies immediate diffusion at an infinite propagation speed (i.e. $c \to \infty$), resulting in an instantaneous, non-zero temperature gradient throughout the medium. With a non-zero value of τ, the thermal wave propagates with a finite wave speed $c = \sqrt{\alpha/\tau}$.

Though the heat flux equation is different for hyperbolic and parabolic heat conduction, the energy equation remains unchanged for both cases. For one-dimensional, planar geometry, the energy equation is given by,

$$-\frac{\partial q(x,t)}{\partial x} + g(x,t) = \rho C_p \frac{\partial T(x,t)}{\partial t} \tag{3}$$

where $g(x,t)$ is the volumetric energy source, ρ is the density, and C_p is the specific heat. The energy source, $g(x,t)$ is taken to be zero for the cases considered here. Equations (1)–(3), subject to appropriate boundary and initial conditions, constitute the complete mathematical formulation of both the hyperbolic and parabolic form of the heat conduction problem.

Attention is now focused on a semi-infinite region $0 < x < \infty$, initially at a uniform temperature T_0. The following two situations are considered here for comparison.

(1) A heat flux $f(t)$ is applied at $x = 0$, while the

NOMENCLATURE

c	speed of propagation
C_p	specific heat
$\mathbf{E}, \mathbf{F}, \mathbf{H}$	vectors defined by equation (8)
f_r	reference wall flux at $x = 0$
$f(t)$	wall flux at $x = 0$
$\mathbf{F}_0$	vector defined by equation (18b)
$F(\xi)$	dimensionless wall flux at $\eta = 0$
$g(x, t)$	energy generation rate per unit volume
G	amplification factor for MacCormack's scheme defined by equation (15)
k	thermal conductivity
n	refractive index
N	conduction-to-radiation parameter defined by equation (11b)
$q(x, t)$	heat flux
$Q(\eta, \xi)$	dimensionless heat flux, $q(x, t)/f_r$
t	time variable
T_0	initial temperature
T_r	reference temperature, $\alpha f_r/kc$
T_∞	constant ambient temperature
$T(x, t)$	temperature
$u(\xi-\eta)$	unit step function
x	space variable.

Greek symbols

α	thermal diffusivity
α_s	surface absorptivity
β	c/α
Δ_2, Δ_3	second and third order correction term, respectively, defined by equation (17)
η	dimensionless space variable, $cx/2\alpha$
θ_∞	dimensionless ambient temperature, T_∞/T_r
$\theta(\eta, \xi)$	dimensionless temperature, $[T(x, t)-T_0]/T_r$
λ	parameter used in equation (19a)
ν	Courant number, $\Delta\xi/\Delta\eta$
ξ	dimensionless time variable, $c^2t/2\alpha$
ρ	density
σ	Stefan–Boltzmann constant
τ	relaxation time, α/c^2.

Subscripts and superscripts

i	spacial location
n	time level.

boundary surface at $x = 0$ dissipates heat by radiation into a medium at T_∞, and the heat transfer is governed by the non-Fourier heat flux equation (1a) and the energy equation (3).

(2) A heat flux $f(t)$ is applied at $x = 0$, while the boundary surface at $x = 0$ dissipates heat by radiation into a medium at T_∞, and the heat transfer is governed by the Fourier heat flux equation (2) and the energy equation (3).

The boundary and initial conditions for both problems are taken as follows:

Initial conditions:

$$T(x, 0) = 0 \tag{4a}$$

$$q(x, 0) = 0 \tag{4b}$$

Boundary conditions:

$$\frac{\partial T(0, t)}{\partial t} = -\frac{1}{\rho C_p}\frac{\partial q(0, t)}{\partial x} \tag{4c}$$

$$q(0, t) = \alpha_s\sigma[T_\infty^4 - T^4(0, t)] + f(t) \tag{4d}$$

$$T(x, t) = 0 \quad x \to \infty \tag{4e}$$

$$q(x, t) = 0 \quad x \to \infty \tag{4f}$$

$$\frac{\partial T(x, t)}{\partial x} = 0 \quad x \to \infty \tag{4g}$$

$$\frac{\partial q(x, t)}{\partial x} = 0 \quad x \to \infty \tag{4h}$$

where $q(x, t)$ is defined by equation (1) for the hyperbolic problem and equation (2) for the parabolic problem.

The hyperbolic problem defined by equations (1) and (3), is now given in the dimensionless form

$$\frac{\partial \theta}{\partial \xi} + \frac{\partial Q}{\partial \eta} = 0 \quad \eta > 0, \quad \xi > 0 \tag{5a}$$

$$\frac{\partial Q}{\partial \xi} + \frac{\partial \theta}{\partial \eta} + 2Q = 0 \quad \eta > 0, \quad \xi > 0 \tag{5b}$$

where the dimensionless time ξ and the dimensionless space variable η are defined as

$$\xi = \frac{c^2 t}{2\alpha} \tag{6a}$$

$$\eta = \frac{cx}{2\alpha} \tag{6b}$$

and the dimensionless temperature $\theta(\eta, \xi)$ and heat flux $Q(\eta, \xi)$ are given by

$$\theta(\eta, \xi) = \frac{T(x, t) - T_0}{\alpha f_r/kc} \tag{7a}$$

$$Q(\eta, \xi) = \frac{q(x, t)}{f_r}. \tag{7b}$$

For the cases studied here, the initial temperature T_0 is taken as zero and f_r is a reference heat flux.

MacCormack's predictor–corrector scheme is used to solve the above hyperbolic problem. To apply this method, the hyperbolic problem defined by (5) is expressed in vector form as

$$\frac{\partial \mathbf{E}}{\partial \xi}+\frac{\partial \mathbf{F}}{\partial \eta}+\mathbf{H}=0 \tag{8a}$$

where

$$\mathbf{E}=\begin{bmatrix}\theta\\ Q\end{bmatrix} \tag{8b}$$

$$\mathbf{F}=\begin{bmatrix}Q\\ \theta\end{bmatrix} \tag{8c}$$

$$\mathbf{H}=\begin{bmatrix}0\\ 2Q\end{bmatrix}. \tag{8d}$$

The parabolic problem defined by equations (2) and (3) is expressed in the dimensionless form as

$$\frac{\partial \theta}{\partial \xi}+\frac{\partial Q}{\partial \eta}=0 \quad \eta>0, \quad \xi>0 \tag{9a}$$

$$\frac{\partial \theta}{\partial \eta}+2Q=0 \quad \eta>0, \quad \xi>0 \tag{9b}$$

where $\xi, \eta, \theta(\eta, \xi)$, and $Q(\eta, \xi)$ are as defined previously. When (9a) and (9b) are combined, the non-dimensional parabolic heat equation is recovered

$$\frac{\partial^2 \theta}{\partial \eta^2}=2\frac{\partial \theta}{\partial \xi}. \tag{10}$$

The solution of equation (10) with a non-linear radiation boundary condition is obtained by using a combined implicit/explicit method.

The dimensionless non-linear boundary condition at $\eta = 0$ for both the hyperbolic and parabolic problems becomes

$$Q(0,\xi)=\frac{\alpha_s}{N}[\theta_\infty^4-\theta^4(0,\xi)]+F(\xi) \tag{11a}$$

where

$$N=\frac{k^4c^4}{n^2\sigma\alpha^4 f_r^3}\equiv\frac{k\beta}{n^2\sigma T_r^3} \tag{11b}$$

$$T_r=\frac{\alpha f_r}{kc}, \quad \beta=\frac{c}{\alpha} \tag{11c, d}$$

$$\theta_\infty=\frac{T_\infty}{T_r}, \quad F(\xi)=\frac{f(t)}{f_r} \tag{11e, f}$$

$F(\xi)$ is taken equal to unity for the cases considered here. The physical significance of the conduction-to-radiation parameter N is better envisioned if it is rearranged as

$$N=\frac{k\beta T_r}{n^2\sigma T_r^4}=\frac{q_{\text{cond}}}{q_{\text{rad}}} \tag{12a}$$

where T_r is the reference temperature and β has units of (length)$^{-1}$. Hence, we conclude that N represents the ratio of conduction to radiation flux. In equation (11a), the value of α_s/N is the parameter that affects the linearity of the problem. Thus, the coefficient multiplying the non-linear term can be regarded as

$$\frac{\alpha_s q_{\text{rad}}}{q_{\text{cond}}}\equiv\frac{\alpha_s}{N}. \tag{12b}$$

Thus, a small value of α_s/N corresponds to a negligible amount of radiative transfer at $\eta = 0$, while a large value of α_s/N implies strong radiation, and hence an extremely non-linear problem. With $\alpha_s/N = 0.0$, there is no radiation, and the boundary condition (11a) becomes linear.

An exact analytic solution is available for the parabolic heat conduction equation in a semi-infinite region $0 \leqslant \eta < \infty$ subject to the boundary condition at $\eta = 0$ obtained from equation (11a) by setting $\alpha_s/N = 0$ and $F(\xi) = 1$. It is given by

$$\theta(\eta,\xi)=2\left[\sqrt{\frac{2\xi}{\pi}}\exp\left(\frac{-\eta^2}{2\xi}\right)-\eta\ \text{erfc}\left(\frac{\eta}{\sqrt{2\xi}}\right)\right]. \tag{13}$$

For the case of the hyperbolic heat conduction equation, an exact solution is also available [11] for constant heat flux boundary condition. Such solutions are used as the base for comparing the effects of surface radiation on temperature distribution in the medium.

NUMERICAL ANALYSIS

The hyperbolic problem considered here involves a discontinuity at the wave front. MacCormack's predictor–corrector scheme has been shown to handle these discontinuities quite well [16]; therefore it is chosen for the present study. This scheme can be characterized as an explicit, second-order accurate, predictor–corrector sequence for the integration of partial differential equations.

Using this method, the finite-difference form of equation (8) becomes

Predictor:

$$\tilde{\mathbf{E}}_i^{n+1}=\mathbf{E}_i^n-\frac{\Delta\xi}{\Delta\eta}(\mathbf{F}_{i+1}^n-\mathbf{F}_i^n)-\Delta\xi\mathbf{H}_i^n \tag{14a}$$

Corrector:

$$\mathbf{E}_i^{n+1}=\frac{1}{2}\left[\mathbf{E}_i^n+\tilde{\mathbf{E}}_i^{n+1}-\frac{\Delta\xi}{\Delta\eta}\left(\tilde{\mathbf{F}}_i^{n+1}-\tilde{\mathbf{F}}_{i-1}^{n+1}\right)-\Delta\xi\tilde{\mathbf{H}}_i^{n+1}\right] \tag{14b}$$

where the subscript i denotes the grid points in the space domain, superscript n denotes the time level, and the tilde denotes the predicted value at time level $n+1$. In the above finite-difference formulation, a forward differencing is used in the predictor, while backward differencing is used in the corrector. In some problems involving moving discontinuities, it may be advantageous to reverse this differencing in order to prevent instabilities.

To establish the stability criteria, the amplification factor G was determined and found to be identical to that of the Lax–Wendroff scheme given by [17]

$$G=1-\nu^2(1-\cos\gamma)-i\nu\sin\gamma \tag{15}$$

where ν is the Courant number and $0 < \gamma < \pi$. Hence the stability criteria becomes

$$\nu = \frac{\Delta\xi}{\Delta\eta} \leqslant 1. \tag{16}$$

However, with the presence of non-linear terms in the problem, it was necessary to use smaller Courant numbers, i.e. the larger the non-linearity, the smaller the value of ν that must be used. As ν is decreased, the number and amplitude of numerical oscillations increase because of increased magnitude of the truncated error terms. The modified equation can be used in such situations to account for the truncated error terms [18]. In this approach, the vectors **E** and **F** in equation (8) are expanded in a Taylor series and the time derivitives higher than one are eliminated. After some manipulation on the derivatives, the modified equation is determined as,

$$\frac{\partial \mathbf{E}}{\partial \xi} + \frac{\partial \mathbf{F}}{\partial \eta} + \mathbf{H} + \frac{\partial}{\partial \eta}\Delta_2 + \frac{\partial}{\partial \eta}\Delta_3 + O(\Delta^4) = 0 \tag{17a}$$

where

$$\Delta_2 = \frac{1}{3!}(\Delta\eta)^2\left[(1-\nu^2)\frac{\partial^2 \mathbf{F}}{\partial \eta^2}\right] \tag{17b}$$

$$\Delta_3 = \frac{1}{4!}(\Delta\eta)^3\left[3\nu(1-\nu^2)\frac{\partial^3 \mathbf{F}}{\partial \eta^3}\right]. \tag{17c}$$

Clearly, for $\nu = 1$, the error terms Δ_2 and Δ_3 vanish and (17a) reduces to the original equation (8a).

The implications of the error terms Δ_2 and Δ_3 in the numerical calculations are as follows. The odd derivative error term involving Δ_2 produces a dispersion effect which distorts the phase relation between the waves and causes oscillations at the wave front. The even derivative term involving Δ_3 introduces a dissipative effect which tends to reduce the gradient of the wave front. Since these terms contain $(\Delta\eta)^2$ and $(\Delta\eta)^3$ coefficients respectively, adjusting the mesh size alters the relative effects of these two phenomena in distorting the wave front.

Calculation of the error terms in the modified equation is important because it is the modified equation that is actually solved when equation (8) is integrated by MacCormack's scheme. If the error terms are significant (i.e. ν much less than one due to large non-linearities) it may be necessary to correct equation (8) to account for them. This is done by subtracting the error terms from (8), which then becomes

$$\frac{\partial \mathbf{E}}{\partial \xi} + \frac{\partial \mathbf{F}_0}{\partial \eta} + \mathbf{H} = 0 \tag{18a}$$

where

$$\mathbf{F}_0 = \mathbf{F} - \Delta_2 - \Delta_3. \tag{18b}$$

When MacCormack's method is applied to equation (18), the resulting modified equation does not contain Δ_2 or Δ_3. In solving (18), some error is expected to be introduced due to the computation of Δ_2 and Δ_3. This additional error is of fourth order for Δ_2 and fifth order for Δ_3 since second-order accurate approximations are used on second- and third-order error terms, respectively. As stated previously, when ν is close to unity, no modified equation correction is necessary, but when ν is much smaller than one, the corrections may prove to be extremely helpful.

The non-linear parabolic problem is solved by a combined implicit/explicit method. The algorithm for this scheme is taken as

$$\theta_i^{n+1} = \theta_i^n + \frac{\Delta\xi}{2(\Delta\eta)^2}[\lambda(\theta_{i-1}^{n+1} - 2\theta_i^{n+1} + \theta_{i+1}^{n+1}) + (1-\lambda)(\theta_{i-1}^n - 2\theta_i^n + \theta_{i+1}^n)]. \tag{19a}$$

The scheme becomes second-order accurate in time, and sixth-order accurate in space when [17, p. 113]

$$\lambda = \frac{1}{2} - \frac{\sqrt{20}}{12}. \tag{19b}$$

RESULTS AND DISCUSSION

The degree of non-linearity of the equations to be integrated is dependent upon the magnitude of α_s/N. As the non-linearity effects the stability of the scheme, the value of the Courant number to be used with MacCormack's method must be adjusted. The five different values of α_s/N considered in this work ranged from 0.0 to 10.0. The case $\alpha_s/N = 0.0$ corresponds to no surface radiation, and for this case, the equations become linear. The radiation effects can be regarded as strong, for example for $\alpha_s/N = 10.0$, and the resulting system is extremely non-linear. As α_s/N is increased from 0.0 to 10.0, the Courant number is decreased from $\nu = 0.98$ to $\nu = 0.33$. With decreasing ν, oscillations in the solution increase, and the use of the modified equation becomes necessary. In this work, the modified equation was used in Fig. 1 for the case $\alpha_s/N = 10.0$, for which ν was taken as $\nu = 0.33$. For $\alpha_s/N = 0.1$, and $\alpha_s/N = 1.0$, a value of $\nu = 0.91$ was found to give good results without use of the modified equation. The modified equation was also used for each of the hyperbolic solutions presented in Figs. 2 and 3 in order to decrease the magnitude of the oscillatory spike at the wave front.

Figure 1 shows the effects of the parameter α_s/N on the variation of the surface temperature $\theta(0, \xi)$ with dimensionless time, ξ for four different values of α_s/N, namely, 0.01, 0.1, 1.0, and 10.0. The results for the non-radiative case (i.e. $\alpha_s/N = 0.0$) are also included. In order to compare the results obtained with the hyperbolic equation against the parabolic solutions, the curves are presented for both cases. The effects of hyperbolic heat conduction diminish after a certain time, and the solutions converge to that obtainable with the parabolic equation. The stronger the surface radiation, the faster the convergence of the solutions. This is due to the overriding effect of radiation with increasing α_s/N, in comparison to conduction. It should

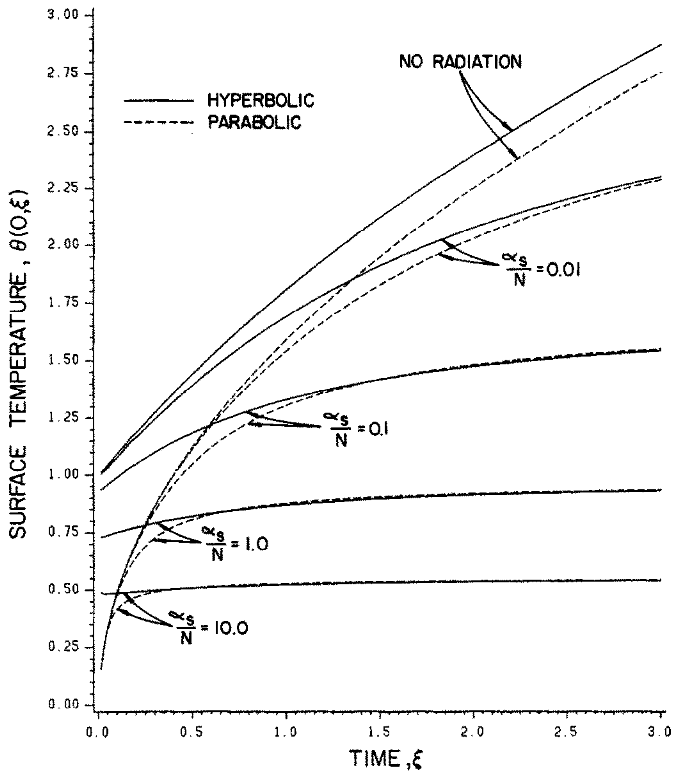

Fig. 1. Effects of boundary radiation on surface temperature.

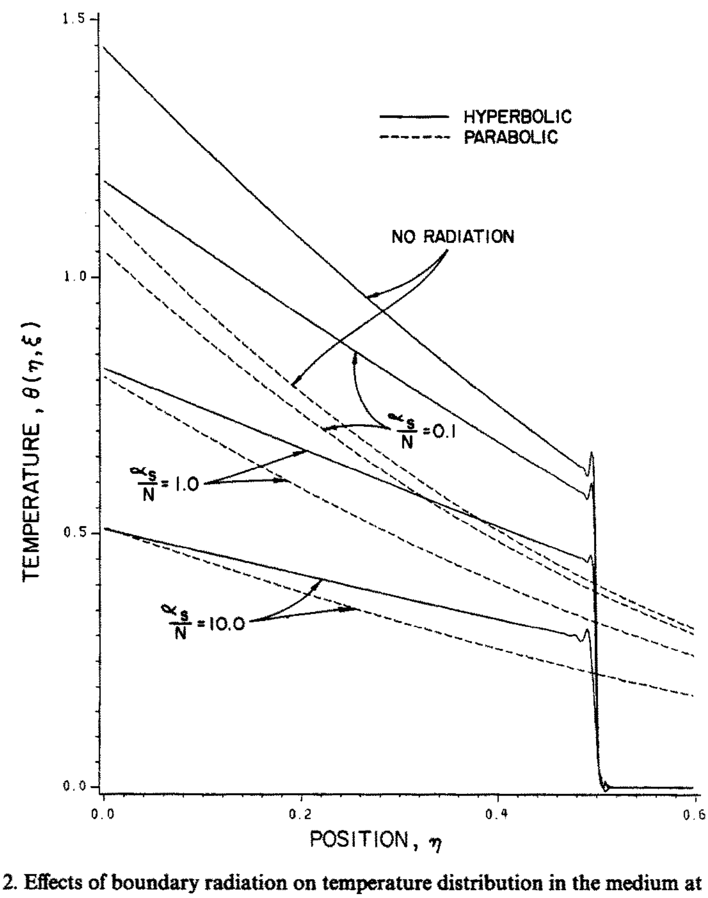

Fig. 2. Effects of boundary radiation on temperature distribution in the medium at $\xi = 0.5$.

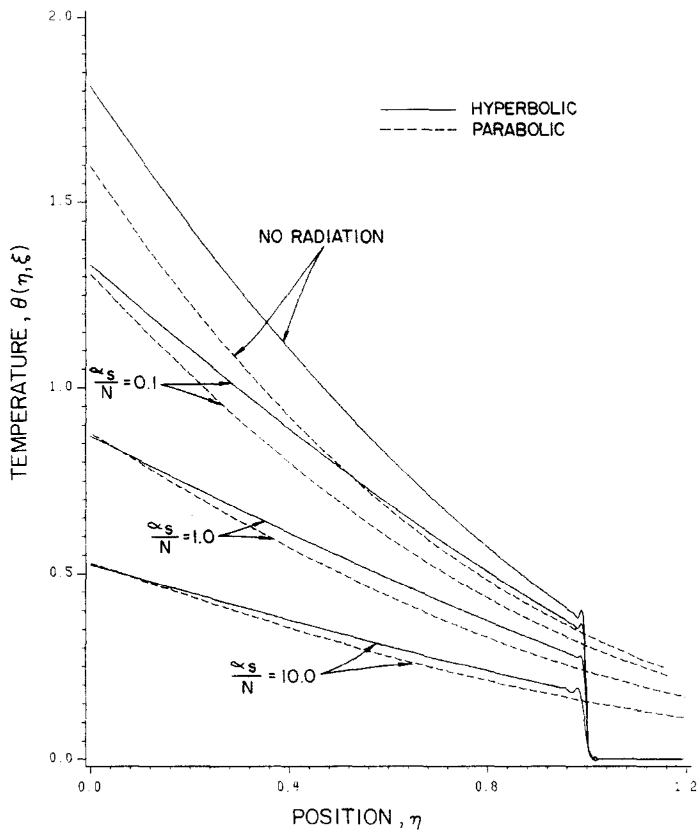

FIG. 3. Effects of boundary radiation on temperature distribution in the medium at $\xi = 1.0$.

be pointed out that the curves in this figure are plotted starting at $\xi = \Delta\xi$, rather than at $\xi = 0.0$. The parabolic solution approaches zero (the initial condition) as ξ goes to zero. However, this is not the case for the hyperbolic problem. When the hyperbolic solution is calculated for very small times, it is seen that the solution converges to some non-zero, finite value. This is consistent with the wave nature of hyperbolic heat transfer, in which there is an instantaneous jump in the surface temperature. This can be seen analytically for the case of no radiation at the boundary where the surface temperature, given by [11]

$$\theta(\eta,\xi) = u(\xi-\eta)\left[e^{-\xi}I_0(\sqrt{\xi^2-\eta^2}) + 2\int_0^{\xi} e^{-\tau}I_0(\sqrt{\tau^2-\eta^2})\,d\tau\right], \quad (20)$$

equals unity as ξ approaches zero.

The hyperbolic solutions presented in this figure include an initial modification to smooth the results. This is done to remove oscillations that occur in the first few time steps due to the discontinuity of the applied flux. The modification involves dividing the first 20 time intervals into subintervals of duration $\Delta\xi/10$. For $\xi > 20\Delta\xi$, the time interval returns to $\Delta\xi$. As an example, consider the case $\alpha_s/N = 0.1$. The solution is calculated from $\xi = 0.0$ to $20\Delta\xi$, using 200 time steps. The solution at the 20 integer values of $\Delta\xi$ are then saved and the solution scheme proceeds, next calculating the solution at $\xi = 21\Delta\xi$. Although this smoothing seems to work quite well, it could not remove all the oscillations for the very non-linear problems. As can be seen in the $\alpha_s/N = 10.0$ curve, the solution shows a slight decrease before it starts a gradual rise.

Figures 2 and 3 show the effects of radiation on temperature distributions in the medium at two different dimensionless times, $\xi = 0.5$ and 1.0, respectively. The results are presented for the values of the parameter $\alpha_s/N = 0.1, 1.0$, and 10.0, as well as for the case of no radiation (i.e. $\alpha_s/N = 0.0$). For comparison purposes, the solutions obtained with the parabolic equations are also presented in this figure. In these figures, 1000 time steps are used to compute the hyperbolic solutions in the time interval between $\xi =$ 0.0 and the final time shown in the figure (i.e. $\xi = 0.5$ for Fig. 2 and $\xi = 1.0$ for Fig. 3), whereas only 200 time steps are used for the parabolic cases. The hyperbolic solutions in both figures are observed to display numerical oscillations at the wave front. These oscillations are due to the dominance of the odd derivative error terms over the even derivative error terms. For example, by multiplying the time step, say, by five, the oscillations could be eliminated, but the gradients at the wavefront would decrease due to the strong dissipative effects. Thus, to ensure a sharp wave front, the smaller time steps are preferred.

As in Fig. 1, we again observe in Figs. 2 and 3, that convergence between the hyperbolic and parabolic solutions occurs more rapidly as the effect of the surface radiation increases. Until convergence is reached, the magnitude of the temperature predicted by the hyperbolic solution is larger than that of the parabolic solution. For the case involving no radiation, this is due to the fact that the total integrated energy in the medium must be equal for the two different types of conduction. When surface radiation is involved, the hyperbolic solution, as a result of the higher surface temperatures, loses more energy due to radiation than the parabolic solution. Thus with increased surface radiation, the difference between the hyperbolic and parabolic temperature profiles, and hence the time to convergence, decrease. In summary, the difference between the hyperbolic and parabolic heat conduction can be simply stated as follows: parabolic heat conduction involves a gradual increase in surface temperature and an infinite rate of energy diffusion, while hyperbolic heat conduction involves an instantaneous increase in surface temperature and a finite rate of energy diffusion. It is this difference that results in temperature variations for extremely short times. As shown above, the time for convergence of the two models is greatly reduced by the presence of surface radiation.

The calculations for all the curves in Fig. 1 required about 25 s in the IBM 3081 computer, while each of the hyperbolic curves in Figs. 2 and 3 required about 83 s. The large amount of time required for Fig. 2 and Fig. 3 is due to the use of a large number of time intervals and the use of the modified equation for reduction of error.

Acknowledgement—This work was supported through the National Science Foundation Grant No. MEA.83 13301.

REFERENCES

1. P. Vernotte, Les panadoxes de la theorie continue de l'equation de la chaleur, *C.r. Acad. Sci. Paris* **246**, 3154–3155 (1958).
2. M. Chester, Second sound in solids, *Phys. Rev.* **131**, 2013–2015 (1963).
3. H. D. Weymann, Finite speed of propagation in heat conduction, diffusion and viscous shear motion, *Am. J. Phys.* **35**, 488–496, 1967.
4. M. E. Gurtin and A. C. Pipkin, A general theory of heat conduction with finite wave speed, *Archs ration. Mech. Analysis* **31**, 113–126 (1968).
5. M. J. Maurer, Relaxation model for heat conduction in metals, *J. appl. Phys.* **40**, 5123–5130 (1969).
6. Y. Taitel, On the parabolic, hyperbolic and discrete formulation of the heat conduction equation, *Int. J. Heat Mass Transfer* **15**, 369–371 (1972).
7. A. V. Luikov, V. A. Bubnov and I. A. Soloview, On the wave solutions of heat conduction equation, *Int. J. Heat Mass Transfer* **19**, 245–248 (1976).
8. V. Peshkov, "Second sound" in helium II, *J. Phys.* **VIII**, 381 (1944).
9. B. Bertman and D. J. Sandiford, "Second sound" in solid helium, *Scient. Am.* **222**, 92–101 (1970).
10. K. J. Baumeister and T. D. Hamill, Hyperbolic heat-conduction equation—a solution for the semi-infinite body problem, *J. Heat Transfer* **191**, 543–548 (1969).
11. M. J. Maurer and H. A. Thompson, Non-Fourier effects at high heat flux, *J. Heat Transfer* **95**, 284–286 (1973).
12. B. Vick and M. N. Özişik, Growth and decay of a thermal pulse predicted by the hyperbolic heat conduction equation, *J. Heat Transfer* **105**, 902–907 (1983).
13. M. N. Özişik and B. Vick, Propagation and reflection of thermal waves in a finite medium, *Int. J. Heat Mass Transfer* **27**, 1845–1854 (1984).
14. D. C. Wiggert, Analysis of early-time transient heat conduction by method of characteristics, *J. Heat Transfer* **99**, 35–40 (1977).
15. G. F. Carey and M. Tsai, Hyperbolic heat transfer with reflection, *Num. Heat Transfer* **5**, 309–327 (1982).
16. D. E. Glass, M. N. Özişik, D. S. McRae and B. Vick, On the numerical solution of hyperbolic heat conduction, *Num. Heat Transfer* (in press).
17. D. A. Anderson, J. C. Tannehill and R. H. Pletcher, *Computational Fluid Mechanics and Heat Transfer*, Chap. 4. Hemisphere, New York (1984).
18. G. H. Klopfer and D. S. McRae, Nonlinear analysis of the truncation errors in finite difference schemes for the full system of Euler equations, AIAA-81-0193, St. Louis, Missouri (January 1981).

CONDUCTION THERMIQUE HYPERBOLIQUE AVEC RAYONNEMENT SUPERFICIEL

Résumé—On utilise une approche numérique pour résoudre la conduction thermique hyperbolique dans un milieu semi-infini où la frontière $x = 0$ est soumise à un flux de chaleur et dissipe la chaleur par rayonnement dans une ambiance à la température T_∞. Les résultats sont comparés à ceux obtenus à partir de l'équation parabolique classique de la chaleur.

HYPERBOLISCHE WÄRMELEITUNG MIT OBERFLÄCHENSTRAHLUNG

Zusammenfassung—Ein numerisches Verfahren wird angewendet, um die hyperbolische Wärmeleitungsgleichung für ein halbunendliches Medium zu lösen, bei dem die Berandung bei $x = 0$ von einem Wärmestrom durchflossen und Wärme durch Strahlung an die Umgebung der Temperatur T_∞ abgegeben wird. Die Ergebnisse werden mit solchen verglichen, die aus der parabolischen Standard-Wärmeleitungsgleichung erhalten wurden.

ГИПЕРБОЛИЧЕСКОЕ УРАВНЕНИЕ ТЕПЛОПРОВОДНОСТИ С ПОВЕРХНОСТНЫМ ИЗЛУЧЕНИЕМ

Аннотация—Численно решается гиперболическое уравнение теплопроводности в полуограниченной среде, в которой граница при $x = 0$ подвержена действию поверхностного теплового потока и отдает тепло в окружающую среду излучением при температуре T_∞. Результаты сравниваются с данными, полученными при решении параболического уравнения теплопроводности.